International Journal of Nanomedicine

Dovepress
open access to scientific and medical research

Open Access Full Text Article

ORIGINAL RESEARCH

EGFR Targeted Cetuximab-Valine-Citrulline (vc)-Doxorubicin Immunoconjugates- Loaded Bovine Serum Albumin (BSA) Nanoparticles for Colorectal Tumor Therapy

This article was published in the following Dove Press journal:
International Journal of Nanomedicine

Zixuan Ye[1,*]
Yue Zhang[1,*]
Yuanfen Liu[2,*]
Yanyan Liu[1]
Jiasheng Tu[1]
Yan Shen[1]

[1]Department of Pharmaceutics, State Key Laboratory of Nature Medicines, China Pharmaceutical University, Nanjing, People's Republic of China; [2]Jiangsu Health Vocational College, Nanjing, People's Republic of China

*These authors contributed equally to this work

Background: Specific modifications to carriers to achieve targeted delivery of chemotherapeutics into malignant tissues are a critical point for efficient diagnosis and therapy. In this case, bovine serum albumin (BSA) was conjugated with cetuximab–valine–citrulline (vc)–doxorubicin (DOX) to target epidermal growth factor receptor (EGFR) and enable the release of drug in EGFR-overexpressed tumor cells.

Methods: Maleimidocaproyl–valine–citrulline–p-aminobenzylcarbonyl-p-nitrophenol (MC-Val-Cit-PAB-PNP) and DOX were used to synthesize MC-Val-Cit-PAB-DOX, which was further linked with cetuximab to prepare antibody–drug conjugates (ADCs). Then, the ADCs were adsorbed to the surface of the BSA nanoparticles (NPs), which were prepared by a desolvation method to obtain cetuximab-vc-DOX-BSA-NPs. The cetuximab-vc-DOX conjugates adsorbed on the surface of the BSA nanoparticles were determined and optimized by size exclusion chromatography. An in vitro cytotoxicity study was conducted using a colon carcinoma cell line with different EGFR-expression levels to test the selectivity of cetuximab-vc-DOX-NPs.

Results: The vc-DOX and cetuximab-vc-DOX conjugates were both synthesized successfully and their structural characteristics confirmed by ^{1}H-NMR and SDS-PAGE. The MTT assay showed stronger cytotoxicity of cetuximab-vc-DOX-NPs versus control IgG-vc-DOX-NPs in EGFR–overexpressing RKO cells. Cellular binding and intracellular accumulation determined by flow cytometry and confocal laser scanning microscopy revealed the strong binding ability of cetuximab-vc-DOX-NPs to RKO cells. The in vivo imaging study demonstrated that cetuximab-vc-DOX-NPs exhibited higher fluorescent intensity in tumor tissues than non-decorated nanoparticles (IgG-vc-DOX-NPs). In vivo tumor inhibition and survival tests showed that cetuximab-vc-DOX-NPs revealed higher tumor inhibition efficacy and lower systemic toxicity than control IgG-vc-DOX- NPs

Conclusion: The obtained results emphasize that cetuximab-vc-DOX-NPs, with good tumor-targeting ability and low systemic toxicity, are a promising targeting system for drug delivery.

Keywords: bovine serum albumin, antibody–drug conjugate, cetuximab, doxorubicin, colonic carcinoma, epidermal growth factor receptor

Correspondence: Yan Shen; Jiasheng Tu
Department of Pharmaceutics, State Key Laboratory of Nature Medicines, China Pharmaceutical University, 24 Tong Jia Xiang, Nanjing, People's Republic of China
Tel +86 25 83271305
Email shenyan@cpu.edu.cn; jiashengtu@aliyun.com

Introduction

Cytotoxic drugs are used to prevent the spread of cancer and are known to kill certain types of cancer cells. The main goal in developing cancer therapeutics is to

identify cytotoxicity against cancer cells to selectively and effectively eradicate tumors without affecting normal tissues.[1,2] Most anticancer drugs currently in use target rapidly dividing cells by disrupting steps in the cell cycle or by targeting the pathways that control normal cell growth and malignant transformation,[3–5] without discriminating between cancer and normal cells. Thus, the major drawback of these conventional cytotoxic drugs is accumulation in normal tissues after administration, which results in serious adverse effects.

One means by which to improve the selectivity and efficacy of cancer therapy is by targeting the altered levels of expression on malignant cells.[1,6,7] Antibody therapy offers many advantages. For example, it specifically targets antigens. Considerable efforts have been made to combine monoclonal antibodies with cytotoxic drugs to reduce the systemic toxicity and increase the therapeutic effect. Antibody–drug conjugates (ADCs), consisting of an antibody carrier and one or multiple drug-linker moieties that conjugate the drug to the antibody carrier, emerged to confer selective and sustained cytotoxic drug delivery to tumors. They can deliver highly potent drugs to targeted cells through specific antibody−antigen binding. The monoclonal antibody of ADCs can highly target antigens expressed on the surface of cells of hematological malignancies and epithelial tumors, thus increasing the accumulation of chemotherapeutics in tumor tissues and cells, followed by enhanced antitumor activity. Recently, two ADC drugs have become available on the market and approved by the FDA, namely, brentuximab vedotin (Adcetris®) for Hodgkin lymphoma and T-DM1 (Kadcyla®) for breast cancer. Colorectal cancer is the third most common type of cancer worldwide and is associated with a poor prognosis.[8] Some colorectal cancer cells express large numbers of epidermal growth factor receptors (EGFRs) on their surface.[9,10] EGFR is a cell-surface receptor tyrosine kinase and member of the EGFR family of extracellular protein ligands.[11] It is involved in the cell cycle and the regulation of cell survival, as well as cellular processes related to metastasis, such as angiogenesis, cell movement, and cell invasion. Many malignancies, including colorectal, head, neck, non-small cell lung, ovarian, breast, and prostate cancers, as well as glioma, overexpress EGFR.[12,13] Therefore, the EGFR is a promising target for cytotoxic drugs for selective chemotherapy. Cetuximab (Erbitux®), which was approved by the FDA for the treatment of colorectal cancer in 2004,[14] is a human–mouse chimeric monoclonal immunoglobulin G_1 (IgG_1) antibody that targets and antagonizes EGF activity, resulting in the induction of apoptosis and the inhibition of cancer cell proliferation.

The linker has a key role in ADC outcomes because its characteristics substantially impact the therapeutic index, efficacy, and pharmacokinetics of the ADC.[15] Stable linkers in ADCs can maintain the antibody concentration in the blood circulation and do not release the cytotoxic drug before reaching the target, resulting in minimum off-target effects. However, the linker should be labile enough to rapidly release the cytotoxic drug once the ADC is internalized to the tumor cells.[16] Previously, it has been well demonstrated that antibody surface-modified nanoparticles with a covalent linkage such as a PEG spacer are specifically internalized in target cancer cells. Comparatively, peptide linkers may offer better control of drug release and also can be selectively cleaved specifically by lysosomal proteases, such as cathepsin B, found in high levels inside tumor cells. Thus, unlike the chemically labile linkers discussed thus far, peptide linkers combine greater systemic stability with rapid enzymatic release of the drug in the target cell.[5]

MC-Val-Cit-PAB-PNP is a cathepsin-cleavable ADC peptide linker. For the FDA-approved drug brentuximab vedotin, the thiols were modified with MC-vc-PAB-MMAE, which incorporates a cathepsin B protease cleavage site (vc: valine–citrulline) and a self-immolative linker (PAB: para-aminobenzyloxycarbonyl) between the maleimide group (MC: maleimidocaproyl) and the cytotoxic drug (MMAE).[17] ADCs containing the Val–Cit linker have been shown to be much more stable in vivo ($t_{1/2}$ for drug release: ~7 days) than previously described hydrazone and disulfide-based linkers.[18]

Despite humanization, cetuximab-containing ADCs still present a potential risk in inducing immunogenicity. As a typical hapten-carrier antigen, an ADC contains two domains, namely, a small molecule compound and the monoclonal antibody (ie, an immunogenic carrier protein). An animal's immune system can recognize the hapten with heterogeneous immune responses, including Ig class-switched high-affinity antibodies.[19,20] This may lead to safety issues, such as anaphylactoid problems of varying severity, and also impact on therapeutic efficacy, rendering the product less effective or non-efficacious. Therefore, it is essential to engineer carrier-loaded ADCs to reduce the immunogenicity and to deliver the cargo to the target cells.

Biologically originating and biodegradable polymers, such as albumin and apolipoprotein-based nanoparticles, are widely used as carriers to deliver drugs because of their specific functions in vivo.[21–23] Owing to the presence of hydrophobic regions, albumin nanoparticles show high affinity toward lipophilic drugs, which can reversibly bind and

allows delivery in the body for release onto or inside the cell (surface or cytoplasm).[24] On the other hand, owing to their high content of charged amino acids, albumin nanoparticles could allow electrostatic adsorption of positively or negatively charged molecules.[25] The secondary structures of albumin contain 48% helical structures and 15% folding structures, while others are random coils, which provide many reticulate interspaces for drug adsorption. In addition, albumin has a favorable pharmacokinetic profile owing to its long half-life in the blood system (19 days).[26] Doxorubicin (DOX) is an effective anticancer drug, which can kill cancer cells by activating apoptosis pathways, but its clinical application is limited because of its serious side effects, especially its inherent dose-dependent cardiotoxicity. It is often loaded into albumin nanoparticles, which can be easily prepared under ambient conditions.[27] For example, Kakinoki and Taguchi introduced a drug delivery system containing DOX; the system was composed of human serum albumin (HSA) and tartaric acid derivative.[28] Bae et al produced DOX-loaded HSA nanoparticles by desolvation.[29] However, these cytostatic drug-loaded nanoparticles may not release drug completely and can induce the death of both cancer cells and normal cells. Thus, in this study, we introduced a drug delivery system combining the advantages of ADCs and albumin nanoparticles to release drug cleavably and specifically without acting in non-target cells such as heart tissue.

In previous studies,[30,31] DOX was loaded in the inner space of bovine serum albumin (BSA) nanoparticles, which resulted in low drug-loading efficiency and non-responsive drug release in the tumor site. Therefore, it is necessary to construct a novel ADC coupling BSA nanoparticles. Since, to the best of our knowledge, there have been no comprehensive reports in the literature on the study of adsorptive attachment of ADCs to BSA nanoparticles, the main objective of this study was to optimize the adsorptive attachment of cetuximab-vc-DOX to BSA nanoparticles and to investigate the cytotoxicity and specific binding of the modified nanoparticles to high and low EGFR-expressing colon carcinoma cells. The preparation and endocytosis of cetuximab-vc-DOX-modified BSA nanoparticles (cetuximab-vc-DOX-NPs) is shown in Figure 1. First, the monoclonal antibody cetuximab was conjugated with DOX by a vc bond. The product was determined qualitatively by sodium dodecyl sulfate–polyacrylamide gel electrophoresis (SDS-PAGE) and high-performance liquid chromatography (HPLC). Then, cetuximab-vc-DOX was adsorptively attached to BSA nanoparticles. The modified BSA nanoparticles produced were further characterized by 3-(4,5-dimethyl-thiazol-2-yl)-2,5-diphenyl-tetrazolium bromide (MTT) assay, flow cytometry (fluorescence-activated cell sorting [FACS]), confocal laser scanning microscopy (CLSM), in vivo imaging in terms of biological reactivity, tumor inhibition efficacy, and survival tests.

Materials and Methods

Materials

MC-Val-Cit-PAB-PNP was purchased from Levena (Nanjing, China), DOX·HCl was obtained from Hisun (Taizhou, China), BSA (purity >97%) was obtained from Xinjingke (Beijing, China), cetuximab was obtained from Merck (Darmstadt, Germany), human IgG antibody was purchased from Yeasen (Shanghai, China), MTT was purchased from Shanghai Institute of Cell Research (Shanghai, China), concanavalin A tetramethylrhodamine was purchased from Invitrogen (Karlsruhe, Germany), cyanine 7-N-hydroxysuccinimide (Cy7-NHS) was purchased from Lumiprobe (New York, USA), and SPF grade BALB/c nude mice, weighing 20–25 g (3 weeks), were obtained from Lingchang (Shanghai, China). All other reagents were of analytical grade and used as received.

Preparation of Cetuximab-vc-DOX Conjugates

Synthesis of MC-Val-Cit-PAB-DOX

MC-Val-Cit-PAB-PNP and DOX·HCl were reacted as previously described. The synthetic pathway is shown in Figure 2.[32] In brief, MC-Val-Cit-PAB-PNP (57.8 mg, 0.1008 mmol) and DOX·HCl (50 mg, 1.1 equivalent) dissolved in N-methyl-2-pyrrolidone (NMP) (4.5 mL) were treated with diisopropylethylamine (DIEA) (0.055 mL, 1.1 equivalent). The mixture was left to stand in the dark at room temperature for 2 days, and then methylene chloride (CH_2Cl_2) (75 mL) was added. The resulting suspension was stored in the freezer overnight, and the solid was collected by filtration and washed with CH_2Cl_2 three times. The undissolved material was purified by flash chromatography on silica gel with a mixture of CH_2Cl_2 and methanol at different ratios: 15:1, 10:1, and 5:1. The sample was loaded at a minimum amount of 2:1 CH_2Cl_2/CH_3OH to produce the product as an orange solid. Then, the product was purified by preparative chromatography (Megres C18, 5 μm, 20×300 mm [Merck, Darmstadt, Germany] 2:1 CH_3OH/50 mM Et_3N/HCO_2H buffer [pH 2.8], flow rate 5 mL/min, λ=280 nm).

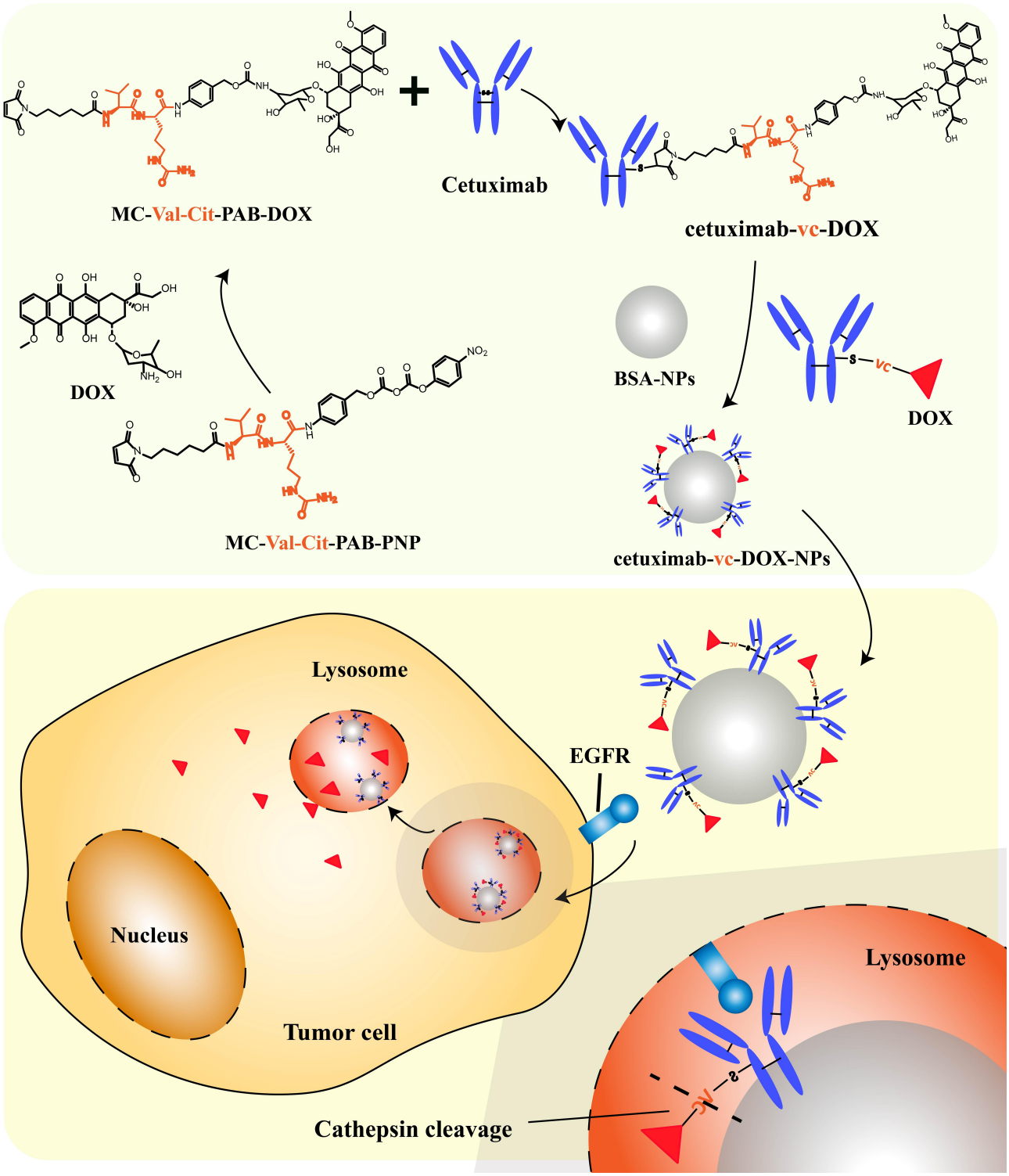

Figure 1 The preparation and endocytosis of cetuximab-vc-DOX-modified BSA nanoparticles (cetuximab-vc-DOX-NPs).

Preparation of Cetuximab-vc-DOX Immunoconjugates (ADCs)

Cetuximab (PBS pH 7.4, 5 mg/mL) was treated with 250 mM sodium borate/250 mM NaCl and 100 mM dithiothreitol (DTT) (pH 8.0), and incubated at 37°C for 45 min. The solution was transferred to a Millipore membrane and diafiltration was carried out against sterile water until cetuximab was totally purified. The concentration of

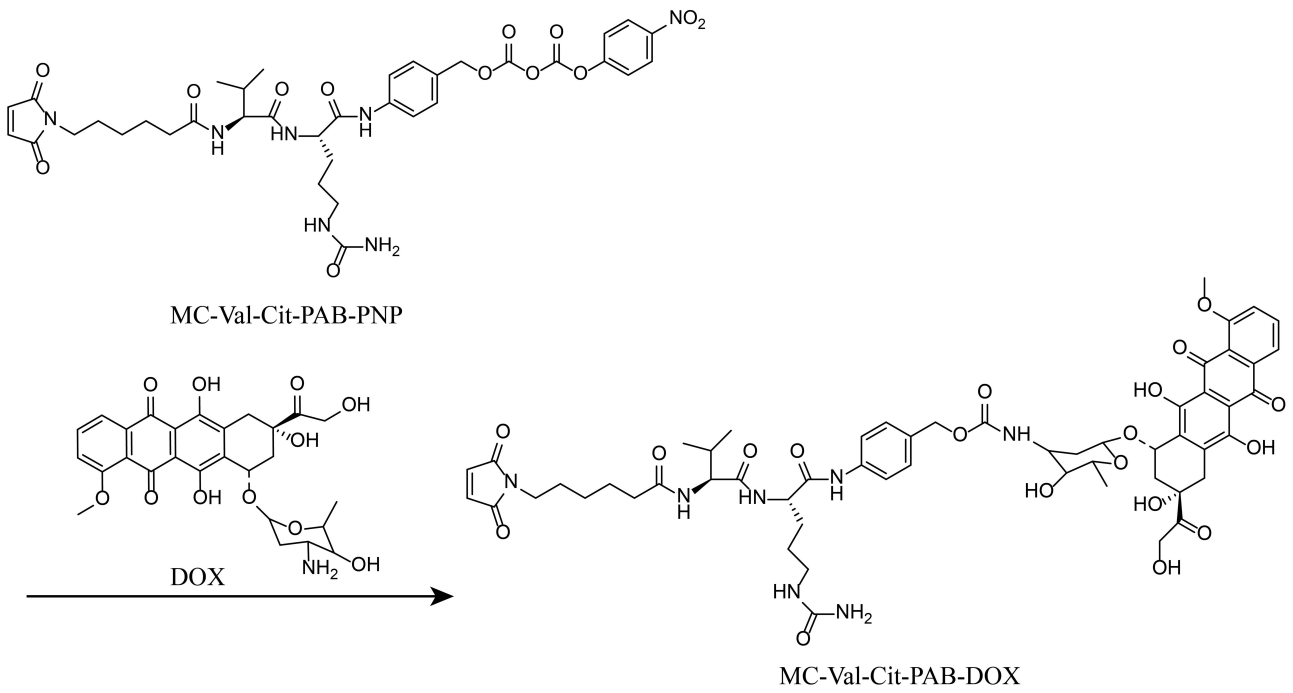

Figure 2 Synthetic pathway of MC-Val-Cit-PAB-DOX.

cetuximab was adjusted to 2 mg/mL, then the solution was treated with MC-Val-Cit-PAB-DOX/DMF (5 mg/mL). After incubation on an ice bath for 1 h, cysteine (PBS, 10 mg/mL) was added to end the reaction in another 45 min. Diafiltration was carried out with sterile water until the effluent was free of SH groups. The human IgG antibody was conjugated with vc-DOX with the same method. The produced IgG-MC-Val-Cit-PAB-DOX (IgG-vc-DOX) was used as the control immunoconjugate.

Characterization of Cetuximab-vc-DOX Conjugates

Characterization of MC-Val-Cit-PAB-DOX

^{1}H-NMR measurements were performed in DMSO-d_6 across the range of 0–15 ppm with a Varian 500 MHz instrument (Bruker, USA). The purity of MC-Val-Cit-PAB -DOX was determined by HPLC (Purospher STAR RP-18 endcapped column [Merck, Germany], 2:1 CH_3OH/50 mM Et_3N/HCO_2H buffer [pH 2.8], flow rate 0.8 mL/min, λ=280 nm). The molecular weight was determined by mass spectrometry using a Waters ZQ 2000 (Waters, USA).

Characterization of Cetuximab-vc-DOX Immunoconjugates

Qualitative Analysis by SDS-PAGE

SDS-PAGE was used to analyze cetuximab-conjugated MC-Val-Cit-PAB-DOX at a constant voltage of 75 V for 30 min, then 115 V for 1.5 h in electrophoresis buffer (0.25 mM Tris, 1.92 mM glycine, 1% SDS, pH 8.3) using a MiniVE (Hoefer, USA) vertical electrophoresis system. The gel was dyed with Coomassie brilliant blue buffer for 1 h, then washed with destaining agent (40% methanol, 7% acetic acid, and 53% water).

Quantitative Analysis of Cetuximab and DOX in Cetuximab-vc-DOX Immunoconjugates

The quantitative analysis of cetuximab and DOX in cetuximab-vc-DOX immunoconjugates was conducted by UV-vis spectrophotometry. A series concentration of DOX·HCl (10–40 μg/mL) was prepared to obtain the standard curve at 495 nm with UV-3200 (Mapada, China), as well as cetuximab (5–1500 μg/mL) at 280 nm, as no absorbance of antibody occurred at 495 nm. Both 280 and 495 nm can be used to determine the absorbance of produced cetuximab-vc-DOX immunoconjugates, followed by calculation of the mole ratio between DOX and cetuximab.

Preparation of BSA Nanoparticles (BSA-NPs)

BSA nanoparticles were prepared by a desolvation method, as described in the literature.[27,33] In brief,

20.0 mg BSA was dissolved in 2.0 mL purified water and the solution was filtered through a 0.22 μm cellulose acetate membrane filter, then the pH was adjusted to 9 with 0.05 M Na_2CO_3-$NaHCO_3$. To form nanoparticles, ethanol was added at the rate of 0.5 mL/min under constant stirring at room temperature. Subsequently, 12 μL of 25% glutaraldehyde solution was added to induce particle cross-linking. The cross-linking was performed under constant stirring of the suspension at room temperature for 16 h. Then, the nanoparticles were purified by centrifugation (15,000 rpm, 15 min, 4°C).

Characterization of Nanoparticles

Determination of Surface-Adsorbed Cetuximab-vc-DOX by SEC

To determine the unbound immunoconjugates, a size exclusion chromatography (SEC) method described previously was used.[34] The resulting supernatants were collected and analyzed by SEC on an Xtimate® SEC-300 column, 7.8 mm × 30 cm (Merck, Germany) using phosphate buffer (pH 7.4) as the eluent, at a flow rate of 0.8 mL/min. Aliquots of 20.0 μL were injected, and the eluent fraction was monitored by detection at 280 nm. To calibrate the SEC system for molecular weight, globular protein standards were used. The amount of cetuximab-vc-DOX bound to the nanoparticle surface was calculated as follows:

$$Loading\ efficiency = \left(\frac{m_0 - c \times V}{m_0}\right) \times 100\%$$

where m_0 represents the amount of cetuximab-vc-DOX added, V represents the total volume of BSA-NP solution and cetuximab-vc-DOX solution, and c is the concentration of cetuximab-vc-DOX determined in the supernatant obtained after the modification step.

Particle Size, Zeta Potential Analysis, and TEM Observation

Nanoparticles were analyzed with regard to zeta potential using a ZetaPlus zeta potential analyzer (Brookhaven Instruments, USA). The particle diameter and polydispersity by photon correlation spectroscopy (PCS) were measured with the same instrument. Prior to both measurements, the samples were diluted with purified water to a suitable concentration. The optimized cetuximab-vc-DOX-NPs was observed by transmission electron microscopy (TEM) (JEOL JEM 1010, Japan).

Cell Cultures

EGFR-overexpressed colorectal cancer cells RKO (ATCC CRL-2577) were purchased from the Type Culture Collection of the Chinese Academy of Sciences (Shanghai, China). The cells were cultured at 37°C and 5% CO_2 in RPMI 1640 medium (Gibco, Invitrogen, Carlsbad, CA, USA) supplemented with 10% fetal calf serum (Gibco Invitrogen) and 1% antibiotics (50 U/mL penicillin and 50 μg/mL streptomycin; Gibco Invitrogen). In addition, EGFR-low-expressed LS174T cells (ATCC CL-188) were used as a control cell line. The cells were cultured at 37°C and 5% CO_2 in DMEM (Gibco Invitrogen) supplemented with 10% fetal calf serum (Gibco Invitrogen) and antibiotics (50 U/mL penicillin and 50 μg/mL streptomycin; Gibco Invitrogen).

Determination of the Cell Viability of Cetuximab-vc-DOX-NPs and IgG-vc-DOX-NPs

The in vitro cell cytotoxicity was assessed on RKO cells and LS174T cells by the MTT assay.[35,36] In brief, 5.0×10^3 cells per well were seeded in a 96-well microplate and incubated at 37°C in a CO_2 incubator for 24 h. After complete cell attachment, the supernatant was removed and the cells were exposed to the different nanoparticle formulations, including DOX, cetuximab-vc-DOX-NPs, and IgG-vc-DOX-NPs (all formulations contained DOX 0.5, 1.5, and 5 μg/mL). BSA-NPs had been proven to be safe, with low cytotoxicity, in our preliminary experiment (data not shown). Control wells were treated with equivalent volumes of culture medium. After incubation, the supernatant was removed and replaced with 200 μL of free medium containing 0.5% fresh MTT solution, and the cells were incubated at 37°C for another 4 h. Then, the medium was discarded and 150 μL of DMSO was added to dissolve the sediment. The microplate was shaken for a moment on a microplate shaker and the absorbance of every well was taken at a wavelength of 490 nm on a multi-scan microplate reader. Cell viability (%) was calculated as follows:

$$Cell\ Viability(\%) = \frac{A_{490}\ of\ treated\ cells}{A_{490}\ of\ control\ cells} \times 100\%$$

Assessment of Cetuximab-vc-DOX-NP and IgG-vc-DOX-NP Binding to EGFR-Positive Cells by Flow Cytometry

The experiment was performed on RKO (EGFR-positive) and LS174T (EGFR-negative) cell lines. After harvesting

the cells by trypsinization and centrifugation (1000 rpm, 5 min), 2×10^5 cells were cultured in six-well plates. After 24 h, the supernatant was removed and the cells were incubated with 2 mL of different nanoparticle formulations (cetuximab-vc-DOX-NPs, IgG-vc-DOX-NPs) in fresh media at 37°C for 4 h and 24 h, which is approximately equivalent to 10 μg/mL of DOX. After this incubation, the cells were washed twice with PBS, then trypsinized and collected. After washing with PBS, flow cytometry (FACS) analysis was performed with 10,000 cells/sample, using a MACSQuant Analyzer (Miltenyi, Germany). The green autofluorescence of these nanoparticles at 488/520 nm showed that this FACS analysis was feasible.

Cellular Uptake and Intracellular Distribution of Cetuximab-vc-DOX-NPs

To investigate the cellular uptake and intracellular distribution of cetuximab-vc-DOX-NPs, the fluorescence accumulation was analyzed using confocal laser scanning microscopy.[37] Thus, 2×10^5 RKO and LS174T cells were seeded into a confocal dish (Becton Dickinson, Germany) and incubated for 4 h at 37°C. Subsequently, the cells were washed twice with PBS, and the membrane was stained with concanavalin A tetramethylrhodamine (50 μg/mL) for 2 min. After fixation with 4% paraformaldehyde (PFA), the cells were washed again with PBS. The confocal microscopy analysis was performed using an LMS 700 device (Zeiss, Germany) equipped with an argon ion laser and LSM Image Examiner software (Zeiss, Germany).[38–40]

Biodistribution of Cy7-Modified Cetuximab-vc-DOX-NPs

To evaluate the in vivo biodistribution and targeting ability of cetuximab-vc-DOX-NPs, amine-reactive Cy7-NHS, a near-infrared (NIR) fluorescent dye, was reacted with BSA-NPs at a ratio of 1:20. Cy7-NHS is a reactive compound suitable for the modification of amino groups on protein, the optimal pH value for modification being 8.3–8.5. Thus, 0.1 M sodium bicarbonate solution was added to the mixture of BSA-NPs and Cy7-NHS to adjust the pH to 8.5, followed by stirring at room temperature for 4 h. The Cy7-labeled BSA-NPs were purified from unreacted Cy7-NHS by diafiltration. A certain amount of the Cy7-modified BSA-NPs was incubated with cetuximab-vc-DOX with a weight ratio of 1.2, as described previously.[41] Finally, the Cy7-modified BSA-NPs were stored at 4°C in the dark until use.

Ethical and legal approval from the Animal Welfare and Research Ethics Committee of China Pharmaceutical University (no 20191105–008) was obtained prior to the start of the animal experiments. All animal experiments were conducted in full compliance with the ethical guidelines of China Pharmaceutical University. Five-week-old SPF-grade BALB/c nude mice (n=8) weighing 20–25 g were implanted with RKO tumor through a subcutaneous injection of 1×10^7 RKO cells suspended in 0.2 mL of Hank's balanced salt solution (HBSS) in the right flank. Tumors were allowed to grow to 1–2 cm in diameter for 2–3 weeks. Cy7-modified nanoparticles were injected into the RKO tumor-bearing mice at a dose of 1.25 mg Cy7/kg via the tail vein to investigate their biodistribution and tumor-targeting efficacy. After injection, images were taken at 1, 2, 4, 6, 8, and 12 h, then the mice were killed and the major organs, including the heart, liver, spleen, lung, and kidney, as well as the tumor, were harvested for imaging.[42,43] An in vivo imaging system (FX PRO; Carestream, Shanghai, China) equipped with an excitation bandpass filter at 750 nm and emission at 780 nm was used to determine the in vivo and in vitro fluorescence intensity. Images were analyzed using the Carestream MI SE (Carestream, China). All experiments were conducted in strict accordance with the National Institute of Health Guide for the Care and Use of Laboratory Animals.

In Vivo Tumor Inhibition and Survival Test

The tumor-bearing mice were equally randomized into three groups (n=6), and every group of mice was treated intravenously with saline, doxorubicin (5 mg/kg), cetuximab (equal to the amount in cetuximab-vc-DOX-NPs), and cetuximab-vc-DOX-NPs (doxorubicin, 5 mg/kg equivalent). The group injected with saline was considered as the control group. The different formulations were injected via the tail vein every 3 days for a total of three times. Recording the first day of administration as day 0, the tumor sizes were determined every other day with a vernier caliper in two dimensions, and calculated as volume $V=d^2\times D/2$ (where D is the long diameter of the tumor and the d is the short diameter perpendicular to the long diameter). The relative tumor volume (RTV) was calculated using the equation $RTV=V_t/V_0$ (where V_t is the volume of tumor determined on day t and V_0 is the volume on day 0). In addition, the body weight and survival rate of the treated mice were monitored every other day.

Statistical Analysis

Statistical analysis was performed using a standard Student's *t*-test (comparing only two individual groups) with a minimum confidence level of 0.05 for significant statistical difference. All values are reported in terms of mean and standard deviation.

Results

Characterization of MC-Val-Cit-PAB-DOX

After synthesis and purification, an orange solid (32.7 mg, 37.5%) was yielded, with a purity of 88%, calculated by the peak area normalization method using HPLC. For ^{1}H-NMR (DMSO) analysis (Figure 3A and B), a characteristic peak appeared at 9.95 ppm, belonging to H (a), peaks at 6.99–8.07 ppm belonged to H (b), and the peak appearing at 5.97 ppm was related to H (c). By electrospray ionization–mass spectrometry, the m/z $(MH)^{+}$ calculated for $C_{56}H_{67}N_7O_{19}$ was 1143.182, and the found value was 1143.7. The ^{1}H-NMR and mass spectrometry results indicated the successful synthesis of MC-Val-Cit-PAB-DOX.

Characterization of Cetuximab-vc-DOX Immunoconjugates

Qualitative Analysis by SDS-PAGE

β-Mercaptoethanol was used as a reducing agent, to reduce the disulfide bond of the antibody and thus split the antibody into light chains and heavy chains. According to the structure of the antibody, the light chain of the antibody can be conjugated with one vc-DOX and the heavy chain can be conjugated with three vc-DOXs. Figure 3B shows that the molecular weight of MC-Val-Cit-PAB-DOX was 1.1 kDa. The results of SDS-PAGE are shown in Figure 3C. It can be seen that the bands of cetuximab and cetuximab-vc-DOX both appear at about 200 kDa, and the light chains and heavy chains of cetuximab are both conjugated with vc-DOX, since two bands appear when cetuximab or cetuximab-vc-DOX is treated with β-mercaptoethanol.

Quantification of Molar Ratio by UV-Vis Spectrophotometry

As shown in Figure 3D and E, the UV absorbance of DOX (10–40 μg/mL) was determined at 495 nm using UV-vis spectrophotometry to obtain three standard curves. Then, the absorbance of cetuximab-vc-DOX was determined at 495 nm to calculate the concentrations of DOX and cetuximab (5–1500 μg/mL) at 280 nm in parallel. The molar ratio of DOX to cetuximab was 5.5.

Surface Modification of BSA-NPs

The particle size of BSA-NPs is 141.5±2.3 nm and the polydispersity index is 0.104 ± 0.024, which indicates the monodisperse distribution of these nanoparticles. The zeta potential is −39.20±1.04 mV.

Equivoluminal cetuximab-vc-DOX adsorbed BSA-NPs were prepared by incubation for 6 h of cetuximab-vc-DOX and BSA nanoparticles at different mass ratios (w/w), ie, 0.4, 0.8, 1.2, and 1.6. Then, the particle size, zeta potential, polydispersity index, and cetuximab-vc-DOX loading efficiency were analyzed, and the results are shown in Table 1. When the ratio increased from 0.4 to 1.2, the particle diameters decreased from 165.1±2.6 nm to 150.9±3.0 nm and cetuximab-vc-DOX loading efficiency increased from 19.0% to 43.9%. However, when the ratio of cetuximab-vc-DOX to BSA-NPs exceeded 1.2, there was no significant difference in particle size and adsorption rate. Therefore, the cetuximab-vc-DOX and BSA nanoparticles prepared with a weight ratio of 1.2 were used for further experiments. The obtained BSA nanoparticles (Figure 4A and B) and cetuximab-vc-DOX-NPs (Figure 4C and D) exhibited a narrow size distribution and round shape.

Meanwhile, an unspecific IgG antibody conjugated with BSA-NPs by the vc linker and unmodified BSA-NPs were prepared as controls following the procedures for cell-culture experiments described in the Materials and Methods section. The physicochemical properties of these three kinds of BSA nanoparticle are summarized in Table 2.

Cell Viability

To assess cytotoxicity, MTT assays were performed for the different formulations using RKO and LS174T cell lines. As shown in Figure 5, both RKO and LS174T cell lines presented a concentration-dependent viability. The measured viability of EGFR-overexpressing RKO cells also decreased after 48 h of incubation for both cetuximab-vc-DOX-NPs and IgG-vc-DOX-NPs, at all concentrations. The strong reduction in viability could be observed at the highest cetuximab-vc-DOX-NP concentration, equivalent to 5 μg/mL DOX. Cetuximab-vc-DOX-NPs had much stronger cytotoxicity than IgG-vc-DOX-NPs, reflecting receptor-mediated uptake. The EGFR-weakly expressing control cell line LS174T showed no changes in viability even after 48 h incubation with cetuximab-vc-DOX-NPs and IgG-vc-DOX-NPs. The cell

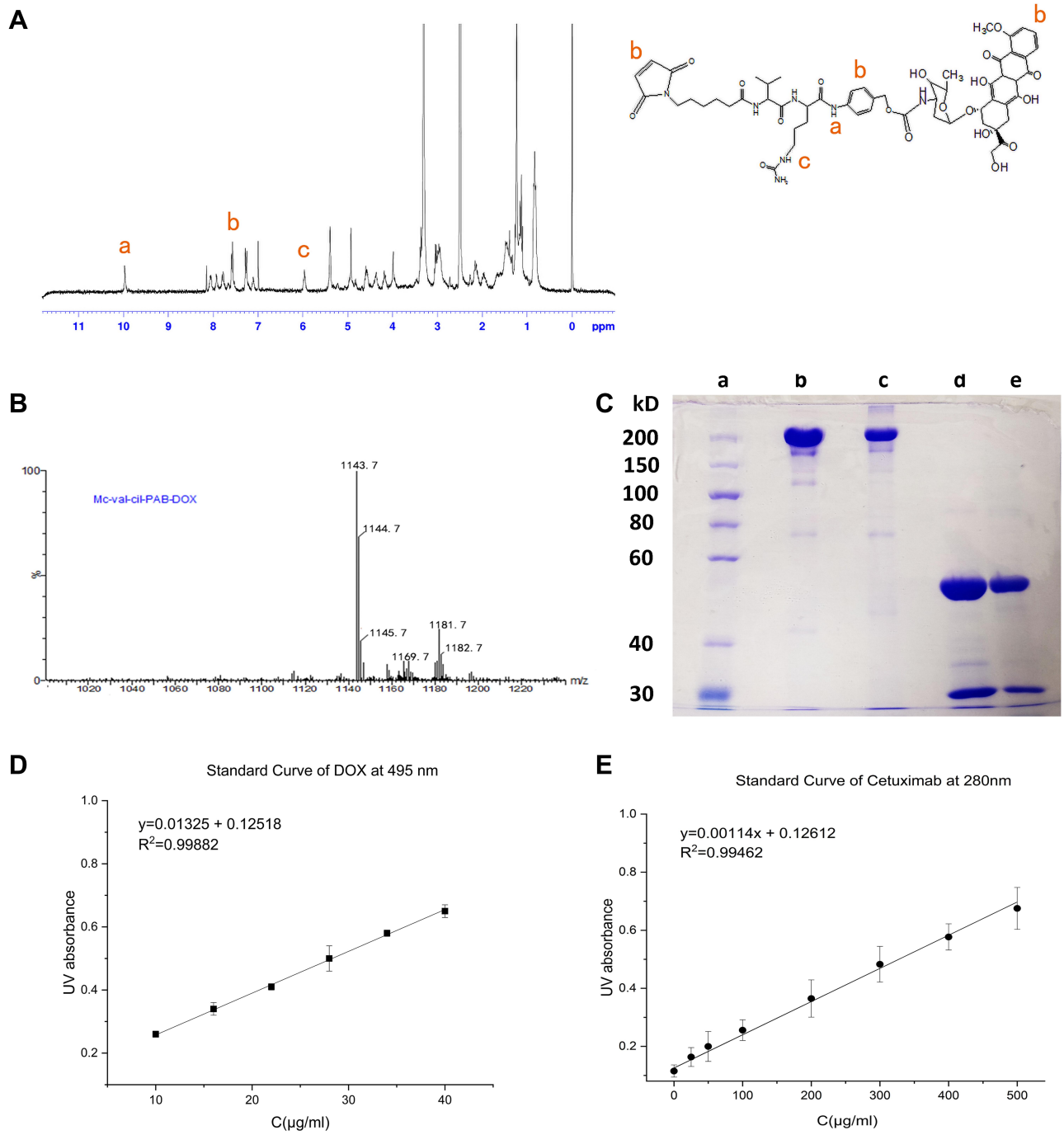

Figure 3 (**A**) ^{1}H-NMR (DMSO) analysis of MC-Val-Cit-PAB-DOX. (**B**) Mass spectrometry results of MC-Val-Cit-PAB-DOX. (**C**) SDS-PAGE analysis of (a) protein marker, (b) cetuximab, (c) cetuximab-vc-DOX, (d) cetuximab treated with β-mercaptoethanol, (e) cetuximab-vc-DOX treated with β-mercaptoethanol. (**D**) Standard curves of DOX (10–40 μg/mL) at 495 nm. (**E**) Standard curves of the monoclonal antibody (5–1500 μg/mL) at 280 nm.

viability of all tested nanoparticles varied marginally for all tested nanoparticles and concentrations. RKO cells are more sensitive to cetuximab-vc-DOX-NPs because of the cetuximab antibody used, which can specifically bind to the EGFR-overexpressed cells.

Assessment of Modified Nanoparticle Binding to EGFR-Positive RKO Cells by Flow Cytometry

The specific binding of the nanoparticulate formulations was analyzed by flow cytometry. Thus, cells were incubated with

Table 1 Physicochemical Characteristics of Different Amounts of Cetuximab-vc-DOX-Modified BSA Nanoparticles (n = 3, Mean ±SD)

Cetuximab-vc-DOX/BSA Nanoparticles (mg/mg)	Particle Diameter (mm)	Polydispersity Index	Zeta Potential (mV)	Cetuximab-vc-DOX Loading (%)
0.4	165.1±2.6	0.160±0.034	−15.2±2.1	19.0
0.8	153.9±1.3	0.090±0.049	−12.1±1.3	40.5
1.2	150.9±3.0	0.151±0.040	−13.3±1.3	43.9
1.6	150.3±2.6	0.110±0.050	−13.9±2.3	44.2

specific cetuximab-vc-DOX-NPs, unspecific control IgG-vc-DOX-NPs, and free DOX for 4 h and 24 h at 37°C. Flow cytometric analysis was performed to quantify their cellular binding.

After 4 h incubation with RKO cells, the free doxorubicin showed the strongest fluorescence, followed by cetuximab-vc-DOX-NPs and IgG-vc-DOX-NPs. There was a significant difference in the percentage of positive cells between cetuximab-vc-DOX-NPs (92.2±14.2%) and IgG-vc-DOX-NPs (69.7±7.8%) (Figure 6) ($p<0.05$). Moreover, the y-geo-mean fluorescence intensities (arbitrary unit) of cetuximab-vc-DOX-NPs and IgG-vc-DOX-NPs were 758±28 and 515±22, respectively ($p<0.01$), reflecting the fact that cetuximab-vc-DOX-NPs could target the EGFR-overexpressed cells. After 24 h incubation with RKO cells, the fluorescence intensity of all formulations declined, especially for the free doxorubicin, from 1207 to 224, which may be due to the drug efflux pump mechanism of the cells. However, the fluorescence intensity of cetuximab-vc-DOX-NPs could be read off from 758 to 312, which showed a reducing effect for drug effluxing to the doxorubicin signals. The possible reason for this is that free doxorubicin can be transported out of the cells by the efflux pumps, but for cetuximab-vc-DOX-NPs, doxorubicin is preserved, probably owing to the cetuximab modification or nanoparticle adsorption. This sustained release effect could help to decrease drug efflux, thus minimizing the doxorubicin dose required for the cancer therapy and lowering the potential toxicity in vivo.[44] Flow cytometric analysis revealed an increased binding of cetuximab-vc-DOX-NPs to RKO compared with LS174T cells. RKO cells showed an increased binding (92.2±14.2%) in comparison with LS174T cells (38.8±5.6%) at 4 h ($p<0.01$), and also (98.1±17.1%) compared

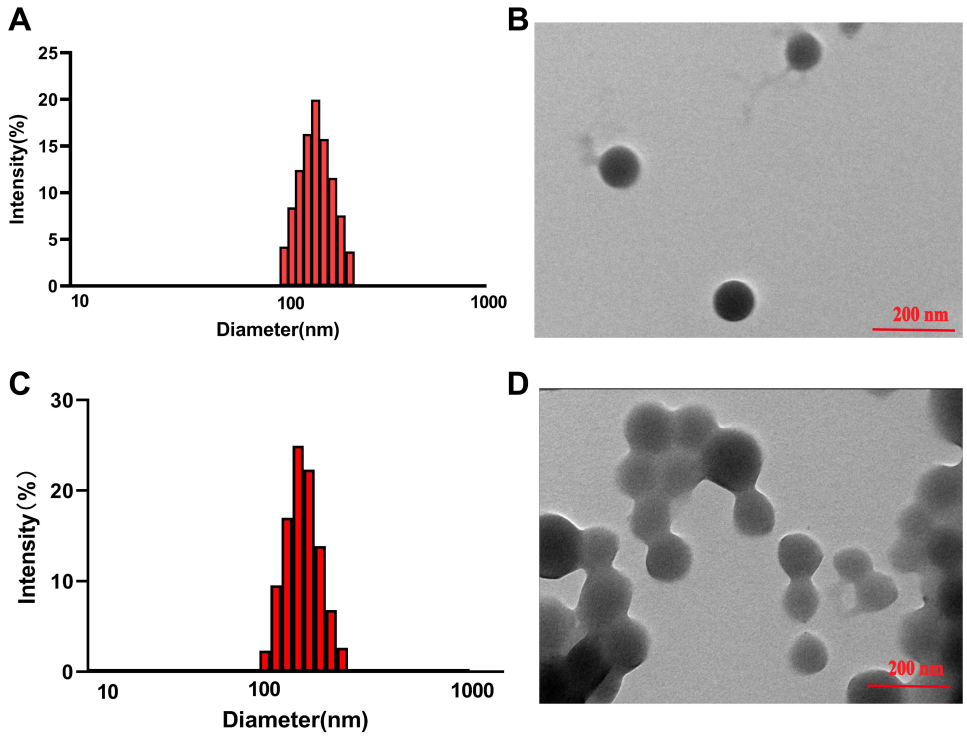

Figure 4 Size distribution by intensity and TEM images of BSA-NPs (**A** and **B**) and cetuximab-vc-DOX-NPs (**C** and **D**).

Table 2 Physicochemical Characteristics of Different Nanoparticles (n = 3, Mean ± SD)

Nanoparticles	Particle Diameter (nm)	Polydispersity Index	Zeta Potential (mV)	Immunoconjugate Loading (%)
Unmodified BSA-NPs	141.5±2.3	0.104±0.024	−29.2±1.04	–
Adsorptive binding of cetuximab-vc-DOX	150.9±3.0	0.151±0.040	−13.3±1.21	43.9
Adsorptive binding of IgG-vc-DOX	206.5±3.5	0.185±0.017	−10.2±1.82	10.5

with LS174T cells (3.5±2.1%) at 24 h ($p<0.01$). Furthermore, the control IgG-vc-DOX-NPs displayed weak binding for both cell lines.

Cellular Uptake and Intracellular Distribution of Nanoparticles

To prove the cellular uptake and in vitro distribution of different nanoparticles, the specific cellular uptake of cetuximab-vc-DOX-NPs was observed by confocal laser scanning microscopy (Figure 7). Cell membranes were observed as red fluorescence after the cells had been stained with concanavalin A tetramethylrhodamine, while DOX was shown as green fluorescence. Co-localization of the DOX with the specific organelle dyes appeared yellow, which indicated that the drug was adsorbed on the surface of the membrane. RKO and LS174T cells were incubated with cetuximab-vc-DOX-NPs. It is shown in Figure 7A that cetuximab-vc-DOX-NPs were accumulated in RKO cells, while almost no cetuximab-vc-DOX-NPs were detected in LS174T cells (Figure 7B), which

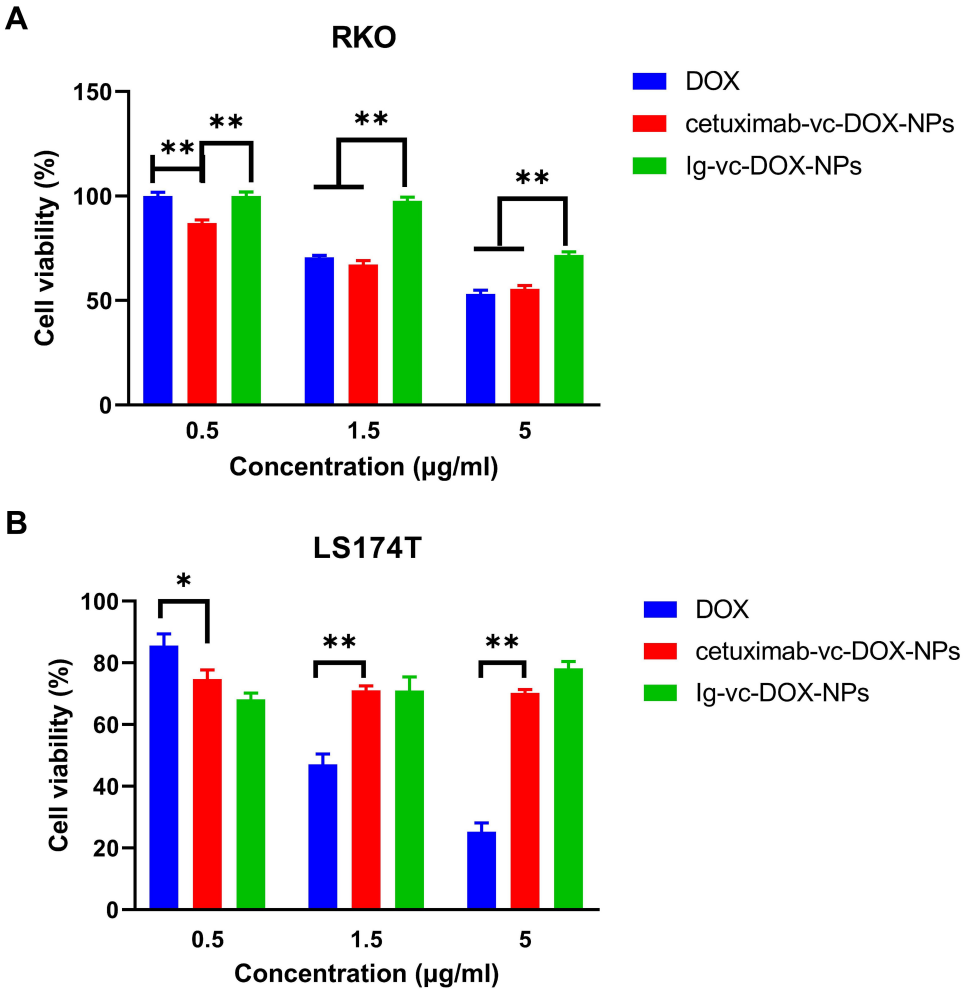

Figure 5 Determination of cell viability (MTT assay). (**A**) RKO and (**B**) LS174T cells were incubated with DOX, cetuximab-vc-DOX-NPs, and IgG-vc-DOX-NPs for 48 h at 37°C. For cetuximab-vc-DOX-NPs and IgG-vc-DOX-NPs, *$p<0.05$, **$p<0.001$.

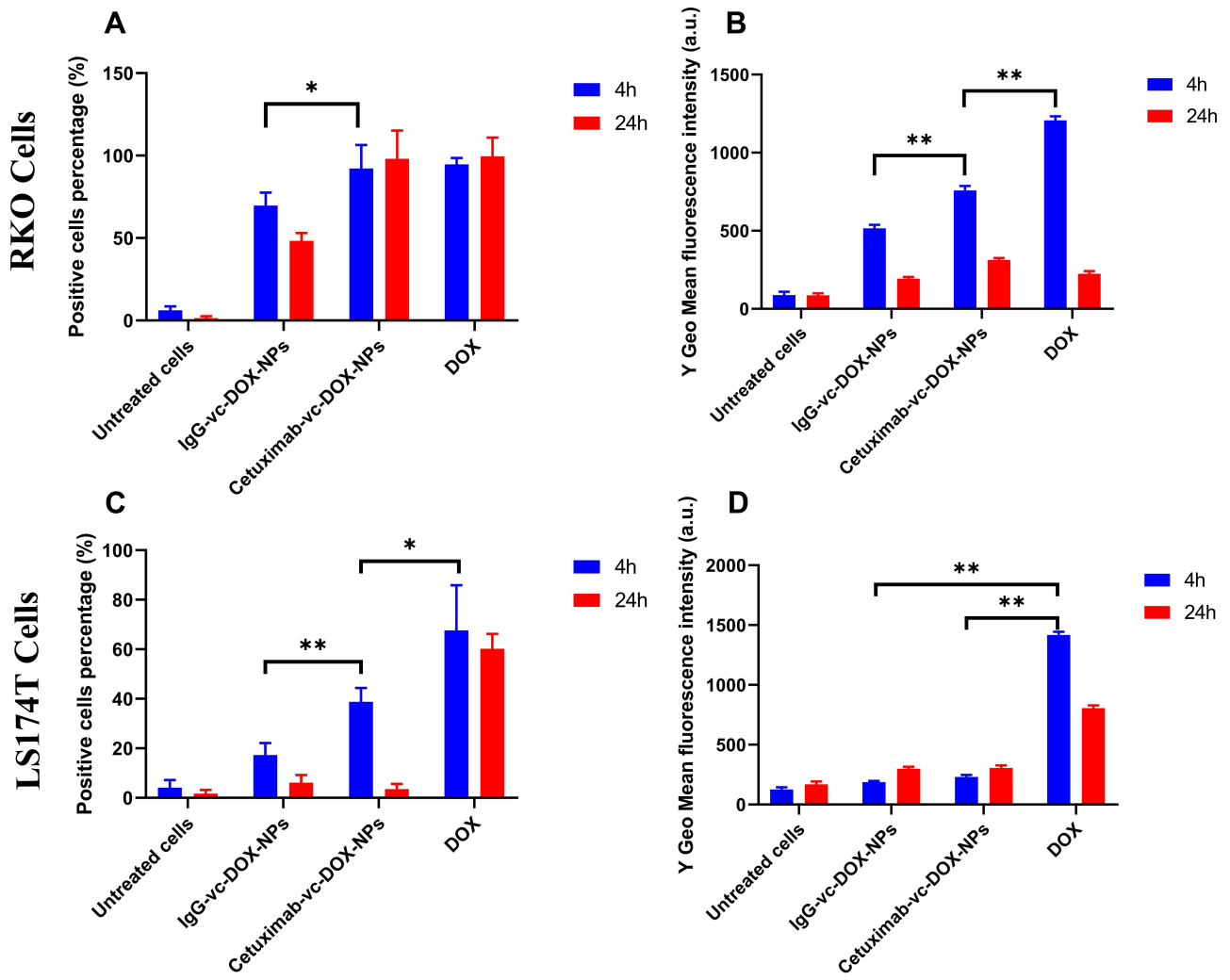

Figure 6 Percentage of positive gated cells (**A** and **C**) and y-geo-mean fluorescence data (**B** and **D**) of different nanoparticles and cells (*p<0.05, **p<0.01).

indicated the specific cellular uptake of cetuximab-vc-DOX-NPs in the EGFR-overexpressing cells.

Biodistribution of ADC Adsorbed Nanoparticles

In this study, a non-invasive near-infrared optical imaging technique was used to image the in vivo biodistribution of Cy7-BSA-NPs and cetuximab-vc-DOX-Cy7-BSA-NPs in RKO tumor-bearing BALB/c nude mice. The mice were treated with different formulations containing Cy7. After 12 h of treatment, the mice were killed and their major organs (heart, liver, spleen, lung, kidney, and brain), including the tumor, were harvested to observe the in vitro fluorescence intensity. Figure 8A shows the real-time images of nanoparticles in the tumor-bearing mice, in which the whole bodies of live mice were monitored at assigned time points, ie, 1, 2, 4, 6, 8, and 12 h after administration. During the live imaging experiment, most of the Cy7 accumulated in the liver and lung after intravenous administration of Cy7-BSA-NPs, with and without cetuximab modification. At 4 h after administration, for the mice injected with control BSA-NPs, the Cy7 accumulation reached a maximum, after which it reduced gradually. The maximum fluorescence intensity of the mice injected with cetuximab-vc-DOX-Cy7-BSA-NPs appeared at 2 h after administration. Moreover, the cetuximab-vc-DOX-modified nanoparticles showed higher tumor-targeting efficiency, which led to higher accumulation in the tumors than control BSA-NPs. This high tumor-target ing ability of nanoparticles may be due to the EGFR-mediated recognition of cetuximab. As shown in Figure 8B, in vitro fluorescent imaging further confirmed that the fluorescence accumulation is higher in the tumors of the cetuximab-vc-DOX-Cy7-BSA-NPs group compared

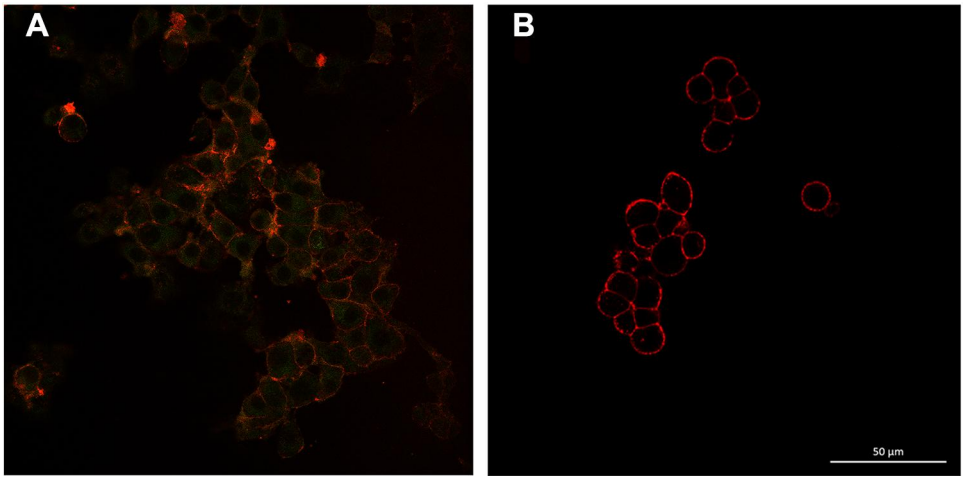

Figure 7 Cellular uptake and intracellular accumulation of surface-modified BSA nanoparticles analyzed by confocal laser scanning microscopy. (**A**) RKO and (**B**) LS174T cells were cultured on a confocal dish and treated with the different nanoparticulate formulations for 4 h at 37°C. The green fluorescence of DOX-loaded nanoparticles was used for detection and the cell membranes were stained with concanavalin A tetramethylrhodamine (red).

with the control group. Besides, the Cy7 accumulation in the liver and lung of the cetuximab-vc-DOX-Cy7-BSA-NPs group was obviously lower than in the control group. In all, in vivo biodistribution studies indicated that cetuximab-vc-DOX-modified BSA-NPs have higher efficiency in targeting EGFR-overexpressing RKO cells than control BSA-NPs, and the results were in accordance with those of in vitro cellular uptake and intracellular distribution.

In Vivo Tumor Inhibition and Survival Test

To investigate and compare the tumor inhibition efficacy of doxorubicin, cetuximab, and cetuximab-vc-DOX-NPs, RKO tumor-bearing nude mice were injected with different formulations via the tail vein. After administration, the mice were weighed and the tumor volumes were examined every other day. The lifetime of the mice was also observed during 40 days. In Figure 9A, the results of the

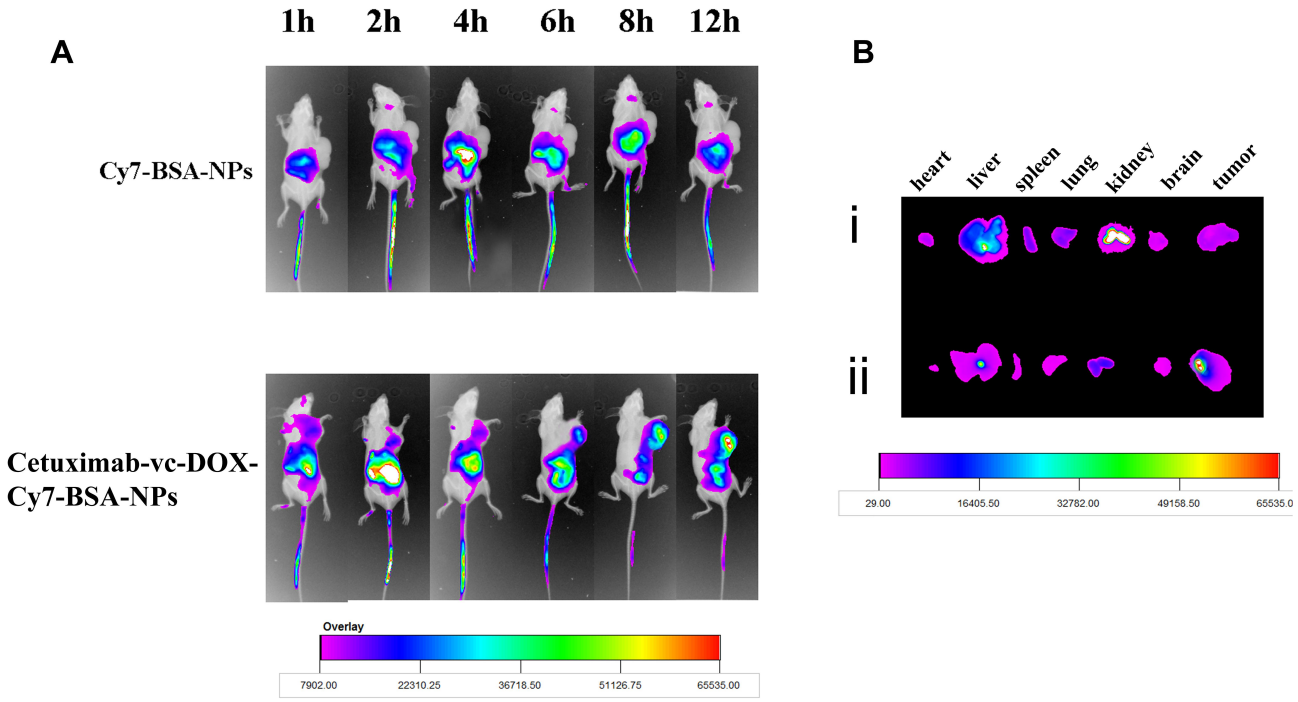

Figure 8 (**A**) In vivo imaging of tumor-bearing mice after administration of Cy7-modified nanoparticles at 1, 2, 4, 6, 8, and 12 h. (**B**) Ex vivo fluorescence images of tissues including heart, liver, spleen, lung, kidney, brain, and tumor collected at 12 h post-injection of (i) Cy7-BSA-NPs and (ii) cetuximab-vc-DOX-Cy7-BSA-NPs.

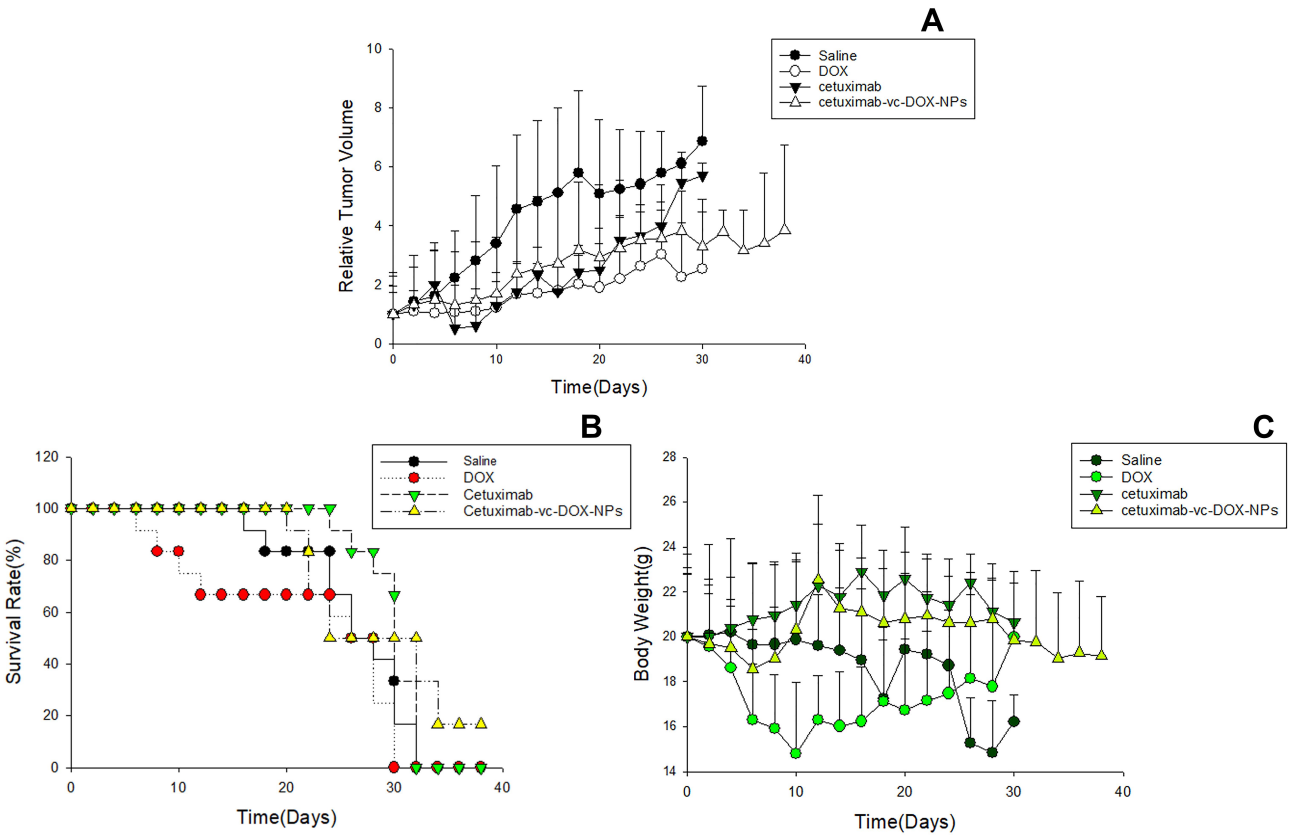

Figure 9 Evaluation of the in vivo inhibition efficacy of treatment with saline, DOX, cetuximab, and cetuximab-vc-DOX-NPs. (**A**) Relative tumor volume of RKO tumor-bearing nude mice (n=6). (**B**) Survival rate of tumor-bearing mice in 38 days. (**C**) Body weight changes of tumor-bearing mice.

antitumor efficacy of saline, doxorubicin, cetuximab, and cetuximab-vc-DOX-NPs are summarized during the course of observation. The control group exhibited no inhibition efficacy on RKO tumors. Compared with the other groups, the cetuximab group showed obvious tumor inhibition effects after the first administration, then the tumor volume increased rapidly, as in the control group. After three administrations, the tumor volume of doxorubicin and cetuximab-vc-DOX-NPs did not show sustainable growth, in contrast to the control group and cetuximab group, which suggests that cetuximab-vc-DOX-NPs and doxorubicin have higher inhibition efficacy on RKO tumors. Since the body weight and lifetime of the mice in this experiment provide a key index to reflect the systemic toxicity of anticancer agents, the body weights and survival rates of the tested groups were monitored (Figure 9B and C). The mice treated with free doxorubicin underwent a significant loss of weight and 20% mice were dead after three administrations, demonstrating that doxorubicin shows acute toxicity in vivo. By comparison, mice treated with cetuximab-modified nanoparticles revealed a small loss of weight, while the weight of the control group showed severe fluctuations. Meanwhile, the mice in the cetuximab-vc-DOX-NPs group could survive for 20 days after administration and 16% of the mice were still alive after 38 days, suggesting that cetuximab-vc-DOX-NPs improved both the inhibition efficacy and the anticancer drug safety.

Discussion

The use of monoclonal antibodies has led to the development of approved biopharmaceutical products in many therapeutic areas, including cardiovascular diseases, infection, immune disorders, and cancer.[45,46] Among these approved products, the humanized IgG_1 monoclonal antibody cetuximab (Erbitux) is directed against the EGFR, which is highly overexpressed in a multitude of cancers.[12,13] The use of cetuximab as a targeting antibody offers the possibility to reach different malignancies, such as head and neck, non-small cell lung, ovarian, breast, prostate, and colorectal cancers.[36] With the development of antibody therapy, antibodies were taken as targeting

ligands with modified and optimized forms to enhance the therapeutic efficiency and reduce the immunogenicity. Significant progress has been made in the ADC field owing to the careful optimization of several parameters, including monoclonal antibody specificity, drug potency, linker technology, and the stoichiometry and placement of conjugated drugs.[47] However, little research has been conducted on attaching ADCs to a carrier, such as nanoparticles, for their potential application.

The goal of this study was to investigate the cytotoxicity of the specific binding and intracellular accumulation of surface-adsorbed BSA nanoparticles along with cetuximab ADCs on two colon carcinoma cell lines with different EGFR-expression levels, ie, RKO with high level and LS174T with low level.[36]

Doxorubicin was modified with a peptide bond using a known method from the literature. The product MC-Val-Cit-PAB-DOX was purified and identified by mass spectrometry and ^{1}H-NMR. Then, the antibody cetuximab was coupled with MC-Val-Cit-PAB-DOX to form the ADC cetuximab-vc-DOX, which was characterized by SDS-PAGE and UV-vis spectroscopy. The unspecific human IgG-vc-DOX was prepared with the same method. The colloid nanoparticle system was formed by the well-known desolvation method.[27,48] Ethanol was added to 1% BSA solution and cross-linked by the addition of 25% glutaraldehyde. Previous studies have demonstrated that antibody surface-modified nanoparticles with a covalent linkage such as PEG spacer are specifically internalized in target cancer cells.[46–48] In the present study, cetuximab-vc-DOX was adsorptively attached to the nanoparticles and the ratio of cetuximab to DOX was optimized. The adsorption resulted in an antibody loading of about 176 μg per mg BSA-nanoparticles by this method.

For the cell culture investigations, the cytotoxicity of the developed nanoparticles was proven by the MTT assay. There was no significant antitumor effect for LS174T cells after incubation for any of the tested nanoparticulate formulations and concentrations. RKO cells demonstrated high sensitivity to cetuximab-vc-DOX-NPs. Consistent with previous findings, cetuximab inhibits the viability of colon carcinoma cells with high EGFR expression but causes no inhibition with low EGFR-expressed cells.[49] Moreover, these results emphasize that the antibody did not demonstrate anticarcinoma activity when adsorptively attached to BSA nanoparticles.

After demonstrating that the developed nanoparticles featured less cytotoxicity, the specific binding efficiency and intracellular accumulation of the different nanoparticle formulations were investigated by flow cytometry. The results of flow cytometry showed that the duration of doxorubicin uptake into cells was elongated by nanoparticles and the drug was more preserved against efflux effects. Therefore, minimization of the needed dose for doxorubicin in cancer therapy is achieved. Concerning the specificity to the tumor site and the minimized drug dose for administration, a reduction of side effects can be expected. Using the cetuximab-vs-DOX conjugates modified to BSA-NPs, the specific accumulation in tumors was improved. Therefore, cetuximab-vs-DOX-NPs are a promising drug carrier system for tumor-targeting drug delivery systems.

From the results of in vivo imaging, it can be concluded that modification with cetuximab-vc-DOX confers BSA nanoparticles with tumor-targeting capability, subsequently decreasing their accumulation in normal organs, ie, liver and lung. These data were also consistent with the results in cellular experiments. To evaluate the in vivo antitumor efficiency, tumor inhibition efficacy and survival tests were conducted. Cetuximab-vc-DOX-modified BSA nanoparticles showed higher antitumor activity than the control group and lower systemic toxicity than doxorubicin.

Conclusion

In conclusion, our ADC-modified nanoparticles can efficiently specifically bind to and internalize in EGFR-overexpressing cancer cells. Owing to the specificity of the system, this nanocarrier could deliver chemotherapy drugs to EGFR-overexpressing tumors, which may lead to a further reduction in systemic toxicity. This study highlights the therapeutic potential of cetuximab-vc-DOX-modified BSA nanoparticles against EGFR-expressing tumors. The combination of a specific targeting antibody and an anticancer drug on a nanoparticulate platform is also a potential strategy for efficient chemotherapy. Further investigations concerning modifications of the antibody and the transport of more anticancer drugs are in progress.

Acknowledgments

This project was supported by the Applied Technology Research and Development Project of the Inner Mongolia Autonomous Region (2019GG035).

Disclosure

The authors report no conflicts of interest in this work.

References

1. Phillips GL. *Antibody-Drug Conjugates and Immunotoxins: From Pre-Clinical Development to Therapeutic Applications*. Springer Science & Business Media; 2012.
2. Sun C, Shen WC, Tu J, Zaro JL. Interaction between cell-penetrating peptides and acid-sensitive anionic oligopeptides as a model for the design of targeted drug carriers. *Mol Pharm*. 2014;11(5):1583–1590. doi:10.1021/mp400747k
3. Bollag DM, McQueney PA, Zhu J, et al. Epothilones, a new class of microtubule-stabilizing agents with a taxol-like mechanism of action. *Cancer Res*. 1995;55(11):2325–2333.
4. Chow K-C, Macdonald TL, Ross WE. DNA binding by epipodophyllotoxins and N-acyl anthracyclines: implications for mechanism of topoisomerase II inhibition. *Mol Pharmacol*. 1988;34(4):467–473.
5. Iyer U, Kadambi V. Antibody drug conjugates—Trojan horses in the war on cancer. *J Pharmacol Toxicol Methods*. 2011;64(3):207–212. doi:10.1016/j.vascn.2011.07.005
6. Wen Y, Kolonich HR, Kruszewski KM, Giannoukakis N, Gawalt ES, Meng WS. Retaining antibodies in tumors with a self-assembling injectable system. *Mol Pharm*. 2013;10(3):1035–1044. doi:10.1021/mp300504z
7. Wen Y, Meng W. Recent in vivo evidences of particle-based delivery of small-interfering RNA (siRNA) into solid tumors. *J Pharm Innov*. 2014;9(2):158–173. doi:10.1007/s12247-014-9183-4
8. Tiwari R, Pandey SK, Goel S, et al. SPINK1 promotes colorectal cancer progression by downregulating Metallothioneins expression. *Oncogenesis*. 2015;4(8):e162–e162. doi:10.1038/oncsis.2015.23
9. Harlé A, Salleron J, Perkins G, et al. Expression of pEGFR and pAKT as response-predictive biomarkers for RAS wild-type patients to anti-EGFR monoclonal antibodies in metastatic colorectal cancers. *Br J Cancer*. 2015;113(4):680–685. doi:10.1038/bjc.2015.250
10. Yang JL, Qu XJ, Russell PJ, Goldstein D. Regulation of epidermal growth factor receptor in human colon cancer cell lines by interferon α. *Gut*. 2004;53(1):123. doi:10.1136/gut.53.1.123
11. Herbst RS. Review of epidermal growth factor receptor biology. *Int J Radiat Oncol Biol Phys*. 2004;59(2):S21–S26. doi:10.1016/j.ijrobp.2003.11.041
12. Mendelsohn J. The epidermal growth factor receptor as a target for cancer therapy. *Endocr Relat Cancer*. 2001;8(1):3–9. doi:10.1677/erc.0.0080003
13. Salomon DS, Brandt R, Ciardiello F, Normanno N. Epidermal growth factor-related peptides and their receptors in human malignancies. *Crit Rev Oncol Hematol*. 1995;19(3):183–232.
14. Wong S-F. Cetuximab: an epidermal growth factor receptor monoclonal antibody for the treatment of colorectal cancer. *Clin Ther*. 2005;27(6):684–694. doi:10.1016/j.clinthera.2005.06.003
15. Hughes B. Antibody-drug conjugates for cancer: poised to deliver? *Nat Rev Drug Discov*. 2010;9(9):665–667. doi:10.1038/nrd3270
16. Teicher BA, Chari RV. Antibody conjugate therapeutics: challenges and potential. *Clin Cancer Res*. 2011;17(20):6389–6397. doi:10.1158/1078-0432.CCR-11-1417
17. Doronina SO, Toki BE, Torgov MY, et al. Development of potent monoclonal antibody auristatin conjugates for cancer therapy. *Nat Biotechnol*. 2003;21(7):778–784. doi:10.1038/nbt832
18. Sanderson RJ, Hering MA, James SF, et al. In vivo drug-linker stability of an anti-CD30 dipeptide-linked auristatin immunoconjugate. *Clin Cancer Res*. 2005;11(2):843–852.
19. Imanishi T, Mäkelä O. Inheritance of antibody specificity I. Anti-(4-hydroxy-3-nitrophenyl) acetyl of the mouse primary response. *J Exp Med*. 1974;140(6):1498–1510. doi:10.1084/jem.140.6.1498
20. Imanishi T, Makela O. Inheritance of fine-specificity in mouse anti-hapten antibodies. Paper presented at: Annales d'immunologie; 1974.
21. Elsadek B, Kratz F. Impact of albumin on drug delivery—new applications on the horizon. *J Controlled Release*. 2012;157(1):4–28. doi:10.1016/j.jconrel.2011.09.069
22. Ding Y, Wang Y, Opoku-Damoah Y, et al. Dual-functional bio-derived nanoparticulates for apoptotic antitumor therapy. *Biomaterials*. 2015;72:90–103. doi:10.1016/j.biomaterials.2015.08.051
23. Ding Y, Wang W, Feng M, et al. A biomimetic nanovector-mediated targeted cholesterol-conjugated siRNA delivery for tumor gene therapy. *Biomaterials*. 2012;33(34):8893–8905. doi:10.1016/j.biomaterials.2012.08.057
24. Kratz F. Albumin as a drug carrier: design of prodrugs, drug conjugates and nanoparticles. *J Controlled Release*. 2008;132(3):171–183. doi:10.1016/j.jconrel.2008.05.010
25. Galisteo-González F, Molina-Bolívar J. Systematic study on the preparation of BSA nanoparticles. *Colloids Surf B Biointerfaces*. 2014;123:286–292. doi:10.1016/j.colsurfb.2014.09.028
26. Elzoghby AO, Samy WM, Elgindy NA. Protein-based nanocarriers as promising drug and gene delivery systems. *J Controlled Release*. 2012;161(1):38–49. doi:10.1016/j.jconrel.2012.04.036
27. Langer K, Balthasar S, Vogel V, Dinauer N, Von Briesen H, Schubert D. Optimization of the preparation process for human serum albumin (HSA) nanoparticles. *Int J Pharm*. 2003;257(1):169–180. doi:10.1016/S0378-5173(03)00134-0
28. Kakinoki S, Taguchi T. Antitumor effect of an injectable in-situ forming drug delivery system composed of a novel tissue adhesive containing doxorubicin hydrochloride. *Eur J Pharm Biopharm*. 2007;67(3):676–681. doi:10.1016/j.ejpb.2007.03.020
29. Bae S, Ma K, Kim TH, et al. Doxorubicin-loaded human serum albumin nanoparticles surface-modified with TNF-related apoptosis-inducing ligand and transferrin for targeting multiple tumor types. *Biomaterials*. 2012;33(5):1536–1546. doi:10.1016/j.biomaterials.2011.10.050
30. Hao H, Ma Q, Huang C, He F, Yao P, et al. Preparation, characterization, and in vivo evaluation of doxorubicin loaded BSA nanoparticles with folic acid modified dextran surface. *Int J Pharm*. 2013;444(1-2):77–84.
31. Kayani Z, Firuzi O, Bordbar AK, et al. Doughnut-shaped bovine serum albumin nanoparticles loaded with doxorubicin for overcoming multidrug-resistant in cancer cells. *Int J Biol Macromol*. 2018;107(Pt B):1835–1843.
32. Dubowchik GM, Firestone RA, Padilla L, et al. Cathepsin B-labile dipeptide linkers for lysosomal release of doxorubicin from internalizing immunoconjugates: model studies of enzymatic drug release and antigen-specific in vitro anticancer activity. *Bioconjug Chem*. 2002;13(4):855–869. doi:10.1021/bc025536j
33. Wei X, Gao J, Fang RH, et al. Nanoparticles camouflaged in platelet membrane coating as an antibody decoy for the treatment of immune thrombocytopenia. *Biomaterials*. 2016;111:116–123. doi:10.1016/j.biomaterials.2016.10.003
34. Kouchakzadeh H, Shojaosadati SA, Tahmasebi F, Shokri F. Optimization of an anti-HER2 monoclonal antibody targeted delivery system using PEGylated human serum albumin nanoparticles. *Int J Pharm*. 2013;447(1):62–69. doi:10.1016/j.ijpharm.2013.02.043
35. Shen Y, Wang J, Li YN, et al. Co-delivery of siRNA and paclitaxel into cancer cells by hyaluronic acid modified redox-sensitive disulfide-crosslinked PLGA-PEI nanoparticles. *RSC Adv*. 2015;5(58):46464–46479. doi:10.1039/C5RA03085D
36. Ling X, Zhao C, Huang L, et al. Synthesis and characterization of hyaluronic acid-platinum (IV) nanoconjugate with enhanced antitumor response and reduced adverse effects. *RSC Adv*. 2015;5(99):81668–81681. doi:10.1039/C5RA16757D
37. Ding Y, Wang Y, Zhou J, et al. Direct cytosolic siRNA delivery by reconstituted high density lipoprotein for target-specific therapy of tumor angiogenesis. *Biomaterials*. 2014;35(25):7214–7227. doi:10.1016/j.biomaterials.2014.05.009

38. Löw K, Wacker M, Wagner S, Langer K, von Briesen H. Targeted human serum albumin nanoparticles for specific uptake in EGFR-Expressing colon carcinoma cells. *Nanomedicine*. 2011;7(4):454–463. doi:10.1016/j.nano.2010.12.003
39. Li C, Li SS, Tu TJ, et al. Paclitaxel-loaded cholesterol-conjugated polyoxyethylene sorbitol oleate polymeric micelles for glioblastoma therapy across the blood-brain barrier. *Polym Chem*. 2015;6(14):2740–2751. doi:10.1039/C4PY01422G
40. Li C, Sun C, Li S, et al. Novel designed polyoxyethylene nonionic surfactant with improved safety and efficiency for anticancer drug delivery. *Int J Nanomed*. 2014;9:2089–2100. doi:10.2147/IJN.S60667
41. Xiong Y, Jiang W, Shen Y, et al. A poly (gamma, L-glutamic acid)-citric acid based nanoconjugate for cisplatin delivery. *Biomaterials*. 2012;33(29):7182–7193. doi:10.1016/j.biomaterials.2012.06.071
42. Balducci A, Wen Y, Zhang Y, et al. A novel probe for the non-invasive detection of tumor-associated inflammation. *Oncoimmunology*. 2013;2(2):e23034. doi:10.4161/onci.23034
43. Ling X, Shen Y, Sun R, et al. Tumor-targeting delivery of hyaluronic acid-platinum (iv) nanoconjugate to reduce toxicity and improve survival. *Polym Chem*. 2015;6(9):1541–1552. doi:10.1039/C4PY01592D
44. Anhorn MG, Wagner S, Kreuter J, Langer K, von Briesen H. Specific targeting of HER2 overexpressing breast cancer cells with doxorubicin-loaded trastuzumab-modified human serum albumin nanoparticles. *Bioconjug Chem*. 2008;19(12):2321–2331. doi:10.1021/bc8002452
45. Nelson AL, Dhimolea E, Reichert JM. Development trends for human monoclonal antibody therapeutics. *Nat Rev Drug Discov*. 2010;9(10):767–774. doi:10.1038/nrd3229
46. Zheng Y, Wen Y, George AM, et al. A peptide-based material platform for displaying antibodies to engage T cells. *Biomaterials*. 2011;32(1):249–257. doi:10.1016/j.biomaterials.2010.08.083
47. Alley SC, Okeley NM, Senter PD. Antibody–drug conjugates: targeted drug delivery for cancer. *Curr Opin Chem Biol*. 2010;14(4):529–537. doi:10.1016/j.cbpa.2010.06.170
48. Weber C, Kreuter J, Langer K. Desolvation process and surface characteristics of HSA-nanoparticles. *Int J Pharm*. 2000;196(2):197–200. doi:10.1016/S0378-5173(99)00420-2
49. Wu X, Fan Z, Masui H, Rosen N, Mendelsohn J. Apoptosis induced by an anti-epidermal growth factor receptor monoclonal antibody in a human colorectal carcinoma cell line and its delay by insulin. *J Clin Invest*. 1995;95(4):1897. doi:10.1172/JCI117871